communications earth & environment

Article

A Nature Portfolio journal

Article in Press

https://doi.org/10.1038/s43247-026-03939-5

Global patterns in small organic particle loss in the mesopelagic ocean

Check for updates

Stephanie Henson[1] ✉, Raphaëlle Sauzède[2], Olivier Aumont[3], Sarah L. C. Giering[1] & Nathan Briggs[1]

The majority of particulate organic carbon in the ocean's mesopelagic zone is contained in particles smaller than 100 μm. However, the challenges of measuring their abundance and carbon content using shipboard techniques has limited our understanding of their role in the ocean carbon cycle. Here we use a 4D Biogeochemical-Argo based data product to investigate the spatial distribution and seasonality in small particles, as well as their loss in the mesopelagic zone. We find that small particle loss in the mesopelagic is greater at high latitudes than at low latitudes. Here we examine several hypotheses that might explain this observed pattern, although limitations in the extant data prevent us drawing definitive conclusions. Contrary to expectations, we find that temperature-driven remineralisation is unlikely to be the primary driver of the observed patterns, and instead find that particle lability may be a significant factor in explaining this unexpected result.

The biological carbon pump (BCP) is the collection of biologically mediated processes that contribute to ocean carbon uptake and storage. Without the BCP, atmospheric CO_2 levels would be ~160 ppm higher than pre-industrial concentrations[1]. Particles sinking and transported from the ocean's upper layer through the mesopelagic are transformed via remineralisation, aggregation, fragmentation, and consumption and egestion by zooplankton[2,3]. Large, rapidly sinking particles are the biggest contributor to the mesopelagic carbon flux[4]. However, small particles can dominate the mesopelagic particle field[5,6] and, although small particles may sink rather slowly (or be suspended), they can still be significant contributors to flux[7–11]. As well as sinking into the mesopelagic, or being transported there by subduction or mesoscale eddies[12], small particles can also be generated at depth by fragmentation of larger particles, either through physical break-up (e.g. shear, turbulence[13]) or biologically-mediated disaggregation (by zooplankton activity[14]). Previous work has suggested that slowly sinking or suspended organic particles could be important as a supply of food to mesopelagic ecosystems[15–17], and that overlooking the role of small particles could exacerbate difficulties in balancing the mesopelagic carbon budget[18–20].

Commonly, particulate organic carbon (POC) reaching 1000 m depth is considered to be sequestered, although the timescales over which sequestration may occur are regionally dependent[21–23]. Nevertheless, the 'transfer efficiency' (T_{eff}), typically quantified as the ratio of POC flux at 1000 m to either the POC flux at 100 m or the base of the euphotic zone, is a convenient and frequently used metric to summarise the efficiency of the BCP[24,25]. Global-scale estimates of T_{eff} have been derived from empirical algorithms applied to satellite data and shipboard observations[26], or by inverse modelling of observed nutrient distributions[27,28]. This has resulted in directly opposing large-scale patterns of T_{eff} being proposed: either high T_{eff} at high latitudes and low T_{eff} at low latitudes[27,29], or vice versa[24,26,30].

One potential explanation for the discrepancy could be that shipboard data syntheses chronically under-sample carbon fluxes, both spatially and temporally, and also tend to be 'clumped' at time series stations or along repeat transects[31]. Furthermore, identifying the distribution of small particles and their importance as a source of POC to the mesopelagic is complicated by the sparsity of data, due to shipboard observations requiring time-consuming filtration of large volumes of water. However, the advent of the BGC-Argo network[32] (https://biogeochemical-argo.org/) offers the potential to overcome some of these sampling biases and has been demonstrated to provide sufficiently dense data coverage to significantly reduce uncertainties in global-scale export flux estimates relative to shipboard sampling[31]. Recent efforts to generate 4D gap-filled, gridded products by combining BGC-Argo data with satellite and/or shipboard observations are enabling new insight into seasonal and interannual variability in biogeochemical processes and greater capacity for validating global biogeochemical models[33–35].

The BGC-Argo network does not, however, measure POC flux directly; instead, the backscatter signal can be used to derive POC concentration with reasonable robustness[36,37]. Here, we investigate the global distribution of small particles (<~100 μm) in the mesopelagic and their potential role in biological carbon cycling using a 4D-resolved dataset of particulate

[1]National Oceanography Centre, European Way, Southampton, UK. [2]Sorbonne Université, CNRS-INSU, FR3761, Institut de la Mer de Villefranche, Villefranche-Sur-mer, France. [3]Sorbonne Université, LOCEAN-IPSL (CNRS-IRD-MNHN-SU), Paris, France. ✉e-mail: s.henson@noc.ac.uk

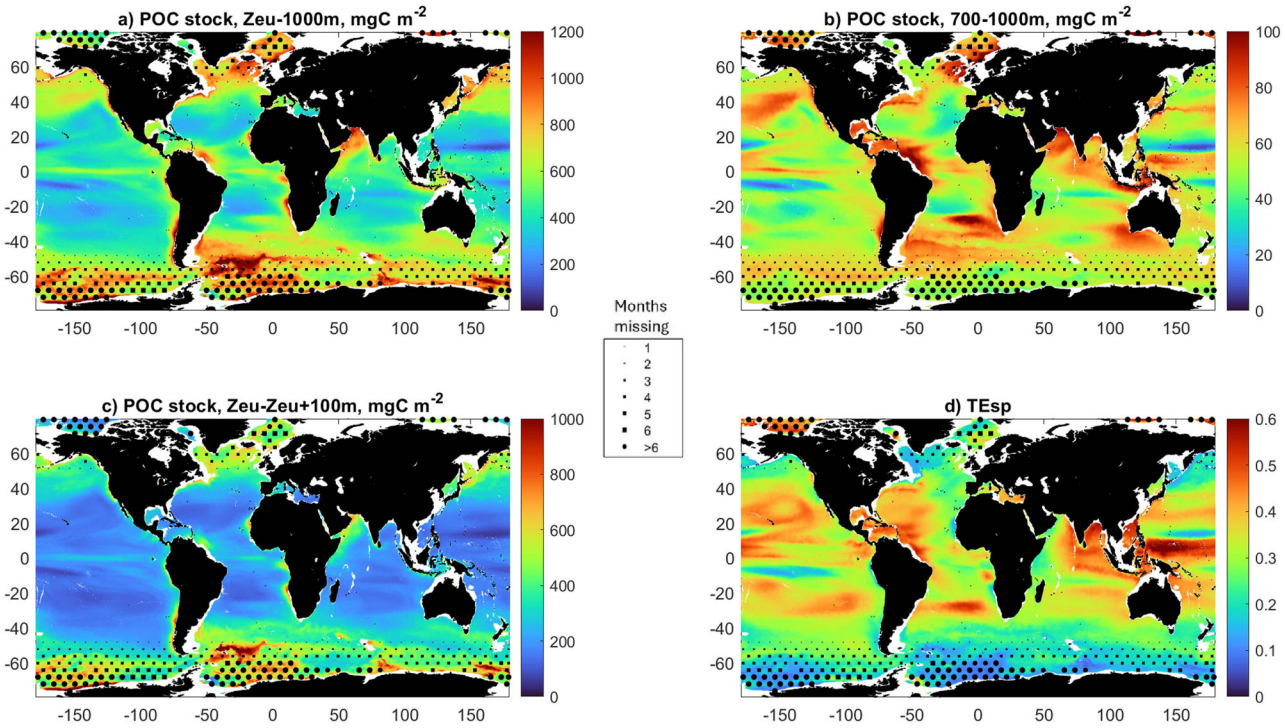

Fig. 1 | Annual mean stock of POC. Annual mean POC stock (mgC m^{-2}) summed over **a** base of euphotic zone to 1000 m, **b** 700–1000 m, **c** base of euphotic zone to 100 m below the euphotic zone, **d** TEsp (ratio of small particle POC at 1000 m to small particle POC at base of euphotic zone). The size of overlaid stippling indicates number of months missing from dataset.

backscattering and POC concentration derived from a machine learning model applied to BGC-Argo and satellite-derived data[38,39].

Results & discussion

POC stocks and ratios

The stock of small particle POC (POCsp) in the mesopelagic is substantial, with highest values at high latitudes (Fig. 1). Comparison with estimates of total annual POC stock suggest that the amount of organic carbon contained in small particles constitutes ~90% of total mesopelagic POC[6]. Substantial concentrations of POCsp also occur in the lower mesopelagic (700–1000 m, Fig. 1b), where the spatial distribution of POCsp is somewhat different than in the upper mesopelagic, with the oligotrophic gyres and upwelling zones less clearly delineated.

Here we use the ratio of annual total POCsp at the base of the euphotic zone to POCsp at 1000 m depth (TEsp) as a simple metric to indicate the change in POCsp stock between the upper ocean and the base of the mesopelagic (Fig. 1d). Using a ratio overcomes the difficulties in attempting to choose a single mathematical function to adequately fit an attenuation curve to a global dataset[40] which increases uncertainty in the results due to the significant variety in the shape of backscatter profiles[41,42]. This approach also has the advantage for our analysis of requiring no assumptions that particles are sinking directly to 1000 m and instead allows for the possibility of particles being generated in the mid-mesopelagic.

The spatial pattern of TEsp (Fig. 1d) demonstrates that the loss of small particles with depth in the mesopelagic is greatest at high latitudes (i.e. TEsp is low; ~10%) and lowest in the oligotrophic gyres (i.e. TEsp is high; ~40%). Although TEsp represents POC concentration, not flux, and only for the small particle fraction, it is nevertheless interesting to note that the spatial pattern of TEsp is similar to that of satellite data-based approaches[26] and inverse to that derived from inverse modelling.

We tested a number of different POC:*bbp* conversion factors using previously published regressions[6,43–46] and found that the spatial patterns in TEsp were not dependent on the choice of conversion equation (although the absolute magnitude changes; Supplementary Fig. 1). Using a ratio between two depths to describe mesopelagic particle loss may overlook vertical variability in the POC profile. To demonstrate that the spatial pattern of TEsp is not unduly affected by this, we calculated TEsp referenced to a range of depths (300, 500 and 700 m; Supplementary Fig. 2). The global spatial pattern of TEsp remains unchanged regardless of the lower depth horizon chosen, implying that this ratio provides a simple and reasonable indicator of particle loss without entailing the uncertainties inherent in attempting to fit an attenuation curve to the data. Moreover, although the uncertainty in POCsp increases with depth, this also does not alter the spatial patterns of TEsp (Supplementary Fig. 3).

Using mixed layer depth as an alternative depth horizon[47] for the upper boundary of TEsp has little impact on the spatial patterns although the absolute magnitude is altered (Supplementary Fig. 4). However, when using a fixed upper boundary of 100 m (rather than the euphotic zone depth as in Fig. 1d), TEsp becomes more uniform with no clear latitudinal trend. At high latitudes, where the euphotic zone is typically shallower than 100 m, using a fixed depth of 100 m to calculate TEsp overlooks the remineralisation occurring immediately below the euphotic depth, resulting in an overestimation of TEsp[48]. In contrast, at low latitudes our results suggest that significant production of small particles is occurring between 100 m depth and the base of the euphotic zone. The difference in the global TEsp patterns due to the choice of export depth underscores the need to consider the implications of different depth horizons for estimates of mesopelagic stocks and fluxes[47].

Drivers of small particle POC distribution

The substantial stock of mesopelagic POCsp confirms that small particles are not necessarily rapidly remineralised as often assumed[49,50], particularly at low latitudes. The spatial pattern in mesopelagic POCsp demonstrates that high latitudes export greater quantities of POCsp than low latitudes, as expected, likely due to their higher productivity, stronger mixing and more significant zooplankton activity compared to low latitudes[51].

Once exported, small particles may reach the mesopelagic through a variety of pathways: sinking from the upper ocean, albeit more slowly than

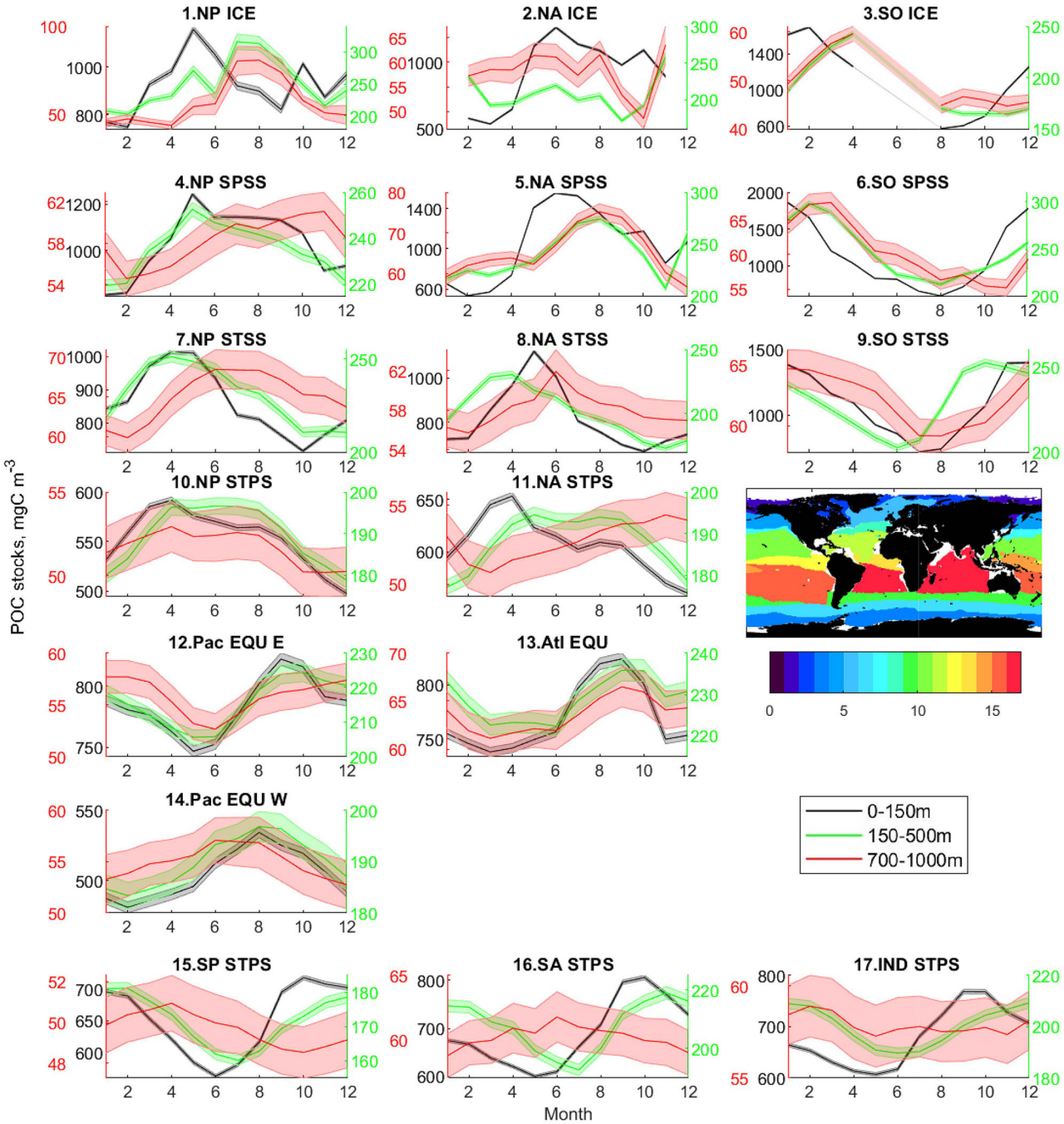

Fig. 2 | Seasonal cycles in biome-averaged POC stocks. POC stocks averaged over layers 5–150 m (black), 150–500 m (green) and 700–1000 m (red). Solid lines show the central estimate of POC stocks and shading indicates the standard error (i.e. σ_{POC} in Eq. (2)). The inset shows the biome map[56]; see Supplementary Table S1 for biome long names.

large particles[9], generation in situ by fragmentation of larger particles[52], or transport into the mesopelagic via physical processes[53–55]. Below, we explore the potential for each of these processes to contribute to the observed patterns in POCsp, although data limitations mean that we are unable to conclusively rule in, or out, any of these hypotheses.

To assess whether particles may be sinking, we investigate the propagation of seasonal peaks in POCsp through depth. The seasonal variability in POCsp stock, averaged per biome[56], is greatest at high latitudes, although the temporal offset between upper and lower mesopelagic POCsp stock varies considerably between regions (Fig. 2). For example, in some regions (e.g. Equatorial Atlantic, Eastern Equatorial Pacific, North Pacific Ice) the seasonal cycles in upper (150–500 m) and lower (700–1000 m) mesopelagic POCsp stock are synchronised. For others (e.g. South Pacific Subtropical Permanently Stratified, North Atlantic and North Pacific Subtropical Seasonally Stratified) there is a clear lag between seasonal peaks in upper and lower mesopelagic POCsp stock, although for some of these regions the magnitude of the seasonal variability at 1000 m is rather small. Although the uncertainty in POCsp increases with depth, the seasonal patterns remain consistent (Fig. 2). A lagged correlation analysis between upper and lower mesopelagic POCsp stocks, grouped by geographical region to overcome the short timeseries (i.e. 12 months), shows that greatest correlation occurs at a lag of 0 months for high latitude biomes and equatorial regions, and a lag of 3 months at low latitudes (Table S2). (Spatially resolved maps of monthly TEsp show a similar seasonality; Supplementary Fig. 5.) We note however

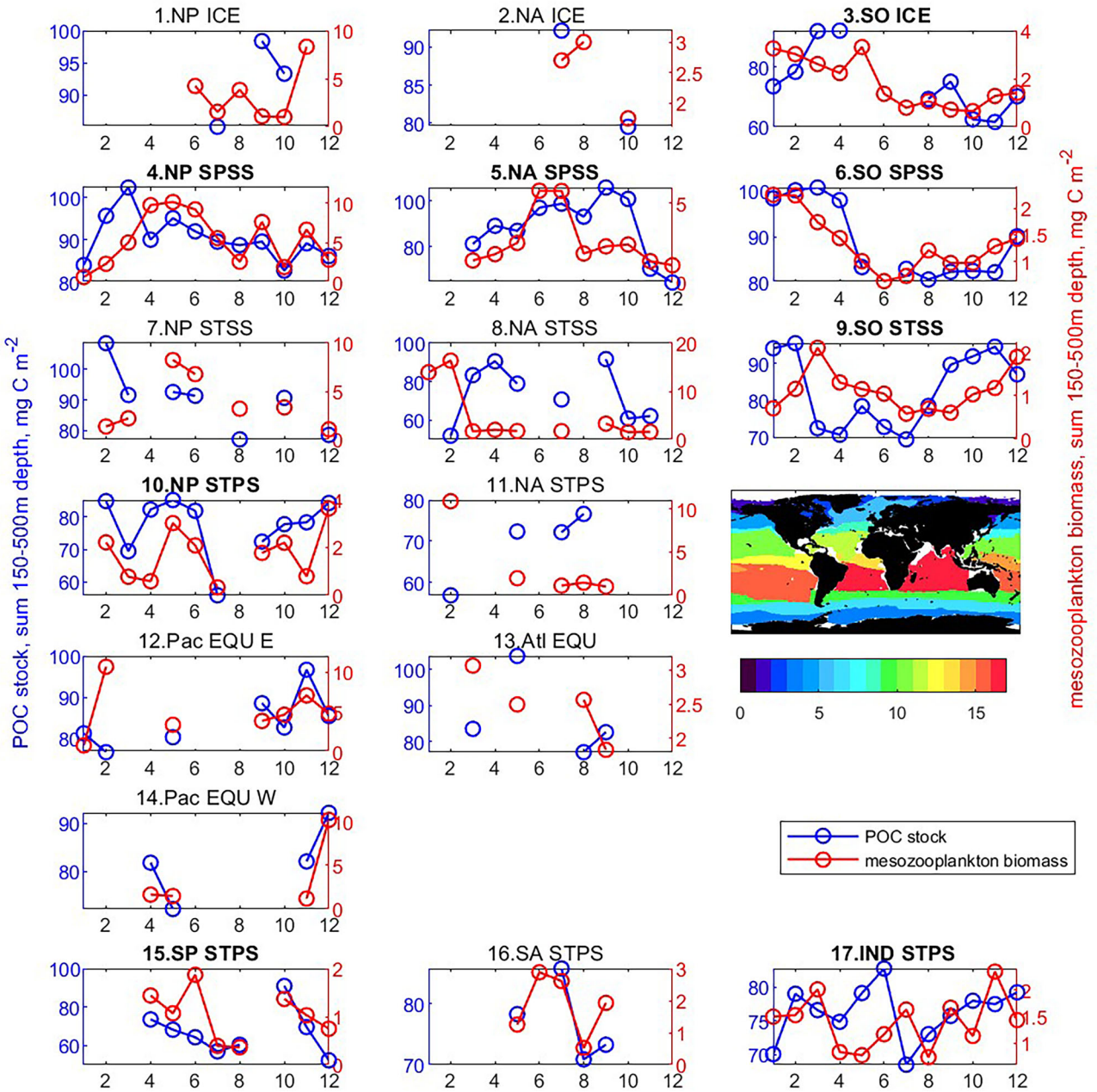

Fig. 3 | Monthly variability in POC stock and mesozooplankton biomass. Monthly time series of POC stock (blue) and mesozooplankton biomass (red) summed over the depth range 150–500 m and averaged into biomes. POC stock data are extracted at the location and month of mesozooplankton samples. Biomes that have sufficient mesozooplankton data to be included in statistical analysis have bold titles. Note the y-axis limits vary across biomes. The inset shows the biome map[56]; see Supplementary Table S1 for biome long names.

that the monthly resolution of the dataset may obscure more rapid fluctuations in POC stocks between the upper and lower mesopelagic, and means that these lag values come with large uncertainty. If we assume that at least a fraction of the small particles may be sinking, these time lags imply POCsp sinking with speeds of ~30 md^{-1} at high latitudes and ~10 md^{-1} at low latitudes. These speeds are consistent with a recent reanalysis of particle size versus sinking speed[57] which suggests a mean sinking speed for particles of 100 μm is ~30 md^{-1}.

Small particles may also be created in situ at mesopelagic depths via fragmentation of large particles by zooplankton activity[14,52]. We compare mesozooplankton biomass from the MAREDAT database[58] with the seasonality in POCsp stock (both integrated over 150–500 m depth) by extracting the POC stock values at the same location and month as all available mesozooplankton samples (Fig. 3). In many biomes and months, few mesozooplankton observations exist (Supplementary Fig. 6) so uncertainties are high. We excluded from further analysis any biomes that had fewer than the median sum of samples across all biomes and less than 6 months of data. Again, to overcome the limitations of performing a lagged correlation analysis on a small sample size, we grouped the timeseries into geographic regions to increase the number of datapoints. In this case, none of the equatorial biomes (and only some of the high latitude and low latitude biomes) had sufficient data to meet our criteria. The results of the lagged correlation analysis on the grouped data is shown in Supplementary Table S3. At high latitudes, mesozooplankton and POC stock correlation is highest for a lag of 0 months, and at low latitudes the mesozooplankton leads POC stock by 2 months. While this apparent correlation does not prove causation, it is suggestive and implies that zooplankton activity, possibly via fragmentation, may result in increased POCsp in the upper mesopelagic.

Finally, small particles may also be passively subducted to mesopelagic depths via the mixed layer pump or eddy-subduction pump[54]. These physical processes are expected to be significant only at high latitudes[53,59] and generally are not the dominant contributor to POC flux, although the mixed layer pump may contribute up to 23% locally in seasonally stratified regions in spring[55]. Although the annual mean TEsp is lower in high latitude regions, the monthly values of TEsp are higher during spring than summer in these regions (Supplementary Fig. 5) suggesting that the mixed layer pump could be a significant source of small particles to the mesopelagic during the winter-spring transition period at high latitudes.

Drivers of small particle TEsp patterns

The spatial pattern in TEsp may be driven by a greater particle loss with depth via higher respiration at high latitudes than low latitudes. This is perhaps surprising, as respiration rates are thought to be greater at warmer temperatures and therefore, all else being equal, a greater loss of POC (i.e. lower TEsp) would be expected in warmer low latitudes. This has generated a long-standing hypothesis that the global spatial pattern of transfer efficiency (of flux in all particle sizes) should be driven by temperature (e.g. ref. 29). The spatial pattern of small particle POC concentration shown here is however opposite, with higher temperatures coinciding with higher TEsp (Fig. 4). We tested both the sea surface temperature and the mean temperature over 150–500 m and found similar patterns (Supplementary Fig. 7). Oxygen may also be a driving factor in setting respiration rate[60], particularly in suboxic zones, however plotting the dissolved oxygen concentration[61] in the range 150–500 m against TEsp revealed no clear patterns (Supplementary Fig. 7d).

As higher temperatures coincide with higher TEsp, factors other than temperature-driven changes in respiration rate must be driving this pattern. An additional hypothesised factor is "sinking-enhanced degradation"[62], which posits that faster-sinking (i.e. likely larger) particles have higher degradation rates than slower-sinking (i.e. likely smaller) particles, due to flow-induced removal of oligomeric breakdown products that compete for enzymatic activity[62]. The study concluded that the sinking-degradation effect, even at relatively modest sinking speeds of 8 md^{-1}, could overcome the temperature effect on degradation rate, so that transfer efficiency was higher than expected, given the temperature, where small particles dominate[62]. This mechanism has so far only been explored in one laboratory study and should be repeated for natural marine particles from a variety of environments to assess its relevance for large scale TEsp patterns.

A possible additional mechanism underlying the unexpected pattern in TEsp lies in the fact that respiration rates are also determined by resource (i.e. food) quality: environments with less labile food are typically associated with lower community respiration rates[63]. Hence, if exported particles are more refractory at low latitudes than their high latitude counterparts, a greater proportion of POCsp could persist in the mesopelagic at low latitudes. A proxy for particle lability that can be derived from BGC-Argo data is the chlorophyll:*bbp* ratio[52,64,65]. Higher values of this ratio are indicative of fresher material, while lower values indicate aged matter. The chlorophyll:*bbp* ratio at 30 m depth is plotted in Fig. 5c and demonstrates that lability proxy values are highest (i.e. fresher material) in northern high latitudes and equatorial regions, and lowest (i.e. more aged material) in oligotrophic gyres. This pattern supports our hypothesis that particle lability plays a role in shaping the observed spatial patterns of TEsp.

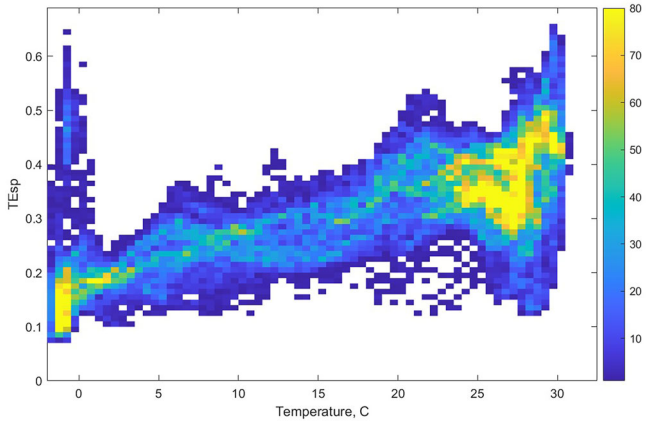

Fig. 4 | Relationship of TEsp and sea surface temperature. Heat map of sea surface temperature plotted against TEsp (ratio of small particle POC at 1000 m to small particle POC at base of euphotic zone), with points coloured by data density. An alternative version of this plot with points coloured by latitude is in Supplementary Fig. 7.

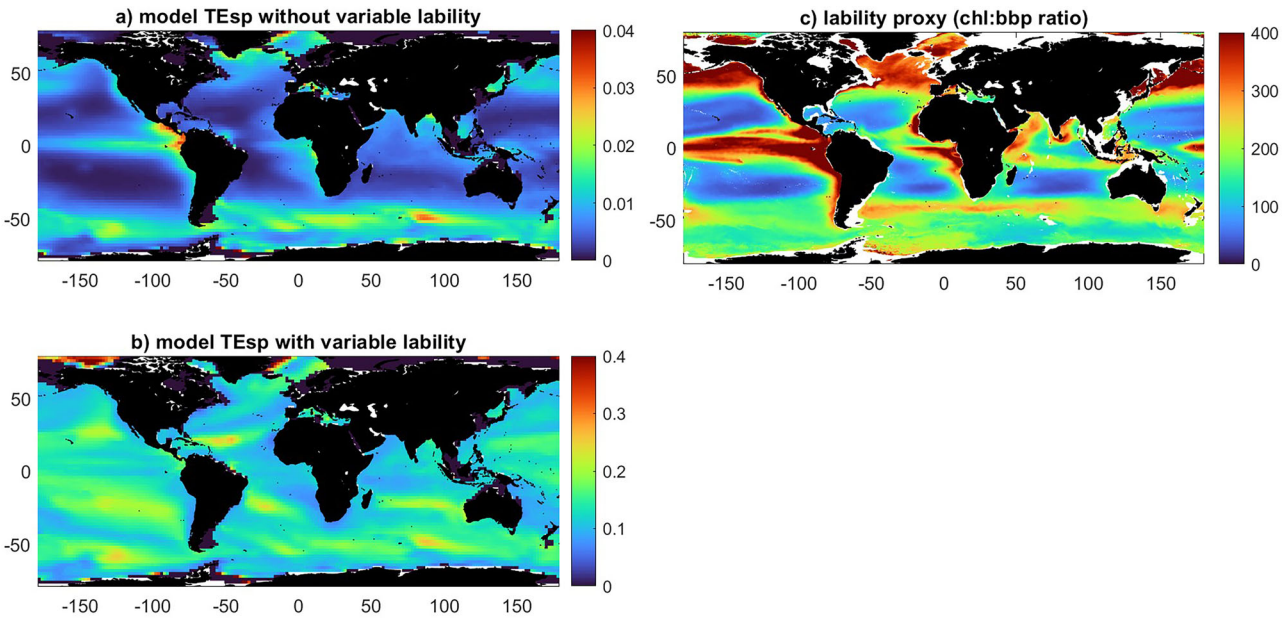

Fig. 5 | Comparison of TEsp in differing model versions and particle lability. TEsp (ratio of small particle POC at 1000 m to small particle POC at base of euphotic zone) from identical model versions[66] without (panel **a**) and with (panel **b**) variable particle lability. Note the different colour scales for the two plots. **c** Proxy indicator for particle lability derived from BGC-Argo data (chlorophyll:*bbp* ratio at 30 m depth), where higher values indicate fresher material and vice versa.

To explore this further, we also investigate the outputs of the PISCES_RC model that incorporates explicit variable particle reactivity (i.e. lability)[66]. We compare the TEsp between the standard model (PISCES_v2) and PISCES_RC (Fig. 5a, b). In PISCES_RC, small particles are predicted to become more refractory at shallower depths than large particles. The high temperatures and thick productive layer typical of oligotrophic regions lead to rapid remineralisation of labile material in the upper ocean[67], so that the remaining fraction that is exported is relatively refractory. As a result, the model without variable particle lability shows a TEsp pattern that is high at high latitudes and low at low latitudes, whereas the model with variable particle lability shows an opposing pattern of higher TEsp in oligotrophic gyres, which much more closely resembles the observed TEsp (compare Fig. 5b and Fig. 1d). It is only the incorporation of variable particle lability that allows the model to approximate the observed TEsp patterns.

Implications

Small particles have generally been understudied, partially due to the challenges of sampling them from shipboard platforms, and partially because the majority of the POC flux is carried in large particles and therefore the assumption follows that small particles are insignificant to mesopelagic carbon cycling. However, the vast majority of mesopelagic organic carbon is held in small particles, which are therefore likely to be an important source of fuel for the metabolism of mesopelagic organisms.

There is a long-standing debate on whether mesopelagic organic carbon supply can meet demand (e.g. ref. 68), although a balance has been demonstrated in some cases[69]. Mesopelagic heterotrophic organisms may be more dependent on the small particle pool than the large, sinking POC to meet their metabolic demands[18–20], particularly in locations or seasons when POC flux is low, e.g. at low latitudes or outside peak bloom periods. Additionally, a recent study has demonstrated that most mesopelagic respiration is not associated with particle-attached microbes on sinking particles, but rather organisms such as zooplankton or free-living bacteria[70]. It seems likely that the slowly sinking (or suspended) particle pool is a critical source of organic carbon for these organisms, in particular for free-living bacteria as it overcomes the problem of a life strategy of being attached to a fast-sinking particle. For zooplankton, the abundance of organic carbon available in small particles is also likely to be an appealing food source due to reduced expenditure of energy in chasing slower-sinking particles[71] and higher encounter rates than for large particles. The high mesopelagic transfer efficiency of small particles at low latitudes demonstrated here implies that POCsp is not heavily consumed and therefore may not make a substantial contribution to interior respiration in low latitudes.

The pattern of TEsp shown here demonstrates that small particles in low latitudes attenuate more slowly with depth in the mesopelagic than expected, implying therefore that these particles are not merely a passive background of non-reactive particles but are being actively reworked or consumed. The main sources of data used to estimate POC flux attenuation (and so sequestration potential) are sediment traps and ^{234}Thorium. Both of these methods are likely to significantly underestimate the contribution of small, slowly sinking particles to potential carbon storage. Although it is generally assumed that sequestration is only possible for large, fast-sinking particles, here we show this is not necessarily the case as a significant fraction of small particles persist even at 1000 m depth. This is especially the case in low latitudes, where small particle respiration could contribute substantially to sequestration in these regions of low POC flux.

Conclusions

Our analysis of small particle POC derived from BGC-Argo data implies that a substantial stock of POC is contained in small particles which we find may be sinking, generated at depth by mesozooplankton activity and/or passively subducted, although we are unable to distinguish their relative contributions in this analysis. We also find that there is reduced loss of small particles in the mesopelagic at low latitudes compared to high latitudes. A possible explanation for this unexpected result is that small particles exported from the upper ocean at low latitudes are more refractory than those exported at high latitudes, which may also be associated with greater ballasting of particles.

Our study suggests that increased attention should be given to the investigation of small particles as, contrary to expectations, they may be significant contributors to energy supply to mesopelagic organisms and may contribute to carbon sequestration in low latitudes. Although here we examine several hypotheses that might explain the observed pattern in small particle loss, limitations in the extant data preclude us from conclusively testing these. To uncover the mechanisms and consequences of small particle dynamics, large-scale data on, for example, mesozooplankton populations, fragmentation rates, particle sinking speeds, particle lability and physical particle injection pumps would be required. Expansion of the deployment of Underwater Vision Profilers (UVP) on BGC-Argo floats would permit widespread data on mesozooplankton distribution and (large) particle morphology to be collected. In combination with the particle backscatter sensors standard on most BGC-Argo floats, this would allow consideration of a size spectrum of particles, broader examination of fragmentation rates and particle sinking speeds via plume tracking. Increasing the number of in situ observations of particle composition and degradation state could help distinguish fresh, labile particles from aged or refractory material, e.g. via amino-acid-based degradation indices, compound-specific or molecular-level mass-spectrometric analyses, or particulate organic matter stoichiometry. Laboratory experiments to quantify how POC lability varies as a function of environmental conditions and source plankton could allow generalisation to larger spatio-temporal scales. Investigating the role of particle injection pumps may require the use of regional models to resolve the necessary scales of variability, with subduction by basin-scale subduction and (sub)mesoscale circulation both potentially contributing to particle dynamics[50,72–74]. Modelling efforts can also be used to scale-up results obtained locally through field studies to global scales and aid in synthesising disparate datasets.

The challenge of observing small particles using shipboard techniques may have slowed understanding of small particle dynamics, however the BGC-Argo network, through new BGC-Argo data-driven gap-filled products, now opens up new possibilities for investigating their significance to mesopelagic carbon cycling.

Methods

The particulate backscattering data product, referred to as SOCA2024, is taken from the Copernicus Marine Service (ref. 39); https://data.marine.copernicus.eu/product/MULTIOBS_GLO_BIO_BGC_3D_REP_015_010/description. This dataset has been produced using satellite-derived data (altimetry and ocean colour) and BGC-Argo measurements of particle backscatter (*bbp*) which have been merged and extrapolated using a machine learning model into a monthly climatology on a 0.25° grid with vertical resolution of 5 m near surface, increasing to 100 m at the maximum depth of 1000 m. The machine learning product has been validated against profile *bbp* data, collected from BGC-Argo floats excluded from the training dataset[38,39]. The SOCA2024 product results in no systematic bias, either spatially or vertically, when compared to the validation *bbp* data with median absolute percent difference of 11% between raw profiles and model output[39]. Seasonal variability in *bbp* is also captured well across differing ocean basins, with the vertical patterns of *bbp* predicted by SOCA2024 being highly consistent with those observed by individual floats[39]. As the backscatter profiles are smoothed vertically to remove spikes[75], the data represent the small particle fraction only (<~100 μm). The spike removal follows an established approach[52], where an 11-point running minimum filter is applied to the profiles, followed by an 11-point running maximum filter. Full details of the dataset, machine learning model and validation can be found in ref. 39. The SOCA2024 dataset averages together multiple BGC-Argo profiles into one grid cell and uses machine learning to produce a gap-free product. For the purposes of our analysis (i.e. a global-scale assessment of spatial patterns in small particles) the processes used to generate this dataset are advantageous as they have the effect of smoothing out episodic

events or the influence of advection which, at finer resolution, may be significant for particle export[43,76].

We convert particulate backscatter (bbp, m^{-1}) to POC concentration (mg C m^{-2}) using Eq. (1)[39], which is derived from a global database of ~6500 POC samples[77]:

$$POC = 66179 * bbp^{1.022} \quad (1)$$

An uncertainty estimate (relative error) for POC is derived using:

$$\frac{\sigma_{POC}}{POC} = \sqrt{\left(\frac{\sigma_A}{A}\right)^2 + \left(\frac{B.\sigma_{bbp}}{bbp}\right)^2 + \left(\ln(\mathrm{bbp}).\sigma_B\right)^2} \quad (2)$$

Where A and B are the conversion factors for bbp to POC; A = 66,179 (±4225) and B = 1.022 (±0.009), where the values in brackets are the 95% confidence limits on the regression coefficients of bbp to POC[39]. In Eq. (2), σ_A and σ_B are the standard errors, i.e. $\sigma_A = 4225/1.96$ and $\sigma_B = 0.009/1.96$. The mapping error (σ_{bbp}) associated with the neural network method used to derive the SOCA2024 bbp product[39] is included in the uncertainty estimate.

In the SOCA2024 dataset, the euphotic zone depth is calculated as the depth where irradiance is reduced to 1% of the surface value and mixed layer depth is calculated as a difference in density of 0.03 kg m^{-3} relative to 10 m depth[78]. Mesozooplankton biomass data were obtained from the MAR-EDAT database[79], which provides biomass data for 11 plankton functional types as global gridded data products (1° × 1° × 33 vertical levels × monthly climatologies)[58]. Sea surface temperature data is the mission composite from the MODIS-Aqua satellite, available from https://oceancolor.gsfc.nasa.gov/, which we regridded to the same spatial and temporal resolution as the SOCA2024 dataset. We also make use of output from a coupled ocean physical and biogeochemical model, PISCES_v2, which is described in full in ref. 80. Two versions of the model are compared: the default version and a version that incorporates a variable particle reactivity continuum[81], PISCES_RC, described in full in ref. 66. An overview of the PISCES_v2 model and the RC version can be found in the Supplementary Information. All analyses were conducted in Matlab R2022a.

Data availability

The small particle backscatter data used in this analysis are available from https://doi.org/10.48670/moi-00046 (ref. 39). The data used to generate the figures is available from https://doi.org/10.5281/zenodo.18418243 (ref. 82).

Code availability

Matlab code used to generate the figures is available from https://doi.org/10.5281/zenodo.18418243 (ref. 82).

Received: 20 February 2026; Accepted: 6 August 2026;
Published online: 20 August 2026

References

1. Tjiputra, J. F., Couespel, D. & Sanders, R. Marine ecosystem role in setting up preindustrial and future climate. *Nat. Commun.* **16**, 2206 (2025).
2. Henson, S. A. et al. Uncertain response of ocean biological carbon export in a changing world. *Nat. Geosci.* **15**, 248–254 (2022).
3. Iversen, M. H. Carbon export in the ocean: a biologist's perspective. *Annu. Rev. Mar. Sci.* **15**, 357–381 (2023).
4. Stemmann, L. & Boss, E. Plankton and particle size and packaging: from determining optical properties to driving the biological pump. *Annu. Rev. Mar. Sci.* **4**, 263–290 (2012).
5. Baker, C. A. et al. Slow-sinking particulate organic carbon in the Atlantic Ocean: magnitude, flux, and potential controls. *Glob. Biogeochem. Cycles* **31**, 1051–1065 (2017).
6. Galí, M., Falls, M., Claustre, H., Aumont, O. & Bernardello, R. Bridging the gaps between particulate backscattering measurements and modeled particulate organic carbon in the ocean. *Biogeosciences* **19**, 1245–1275 (2022).
7. Alonso-González, I. J. et al. Role of slowly settling particles in the ocean carbon cycle. *Geophys. Res. Lett.* **37**, L13608 (2010).
8. Amaral, V. J. et al. Particle cycling rates at Station P as estimated from the inversion of POC concentration data. *Elem. Sci. Anthr.* **10**, 00018 (2022).
9. Durkin, C. A., Estapa, M. L. & Buesseler, K. O. Observations of carbon export by small sinking particles in the upper mesopelagic. *Mar. Chem.* **175**, 72–81 (2015).
10. Simon, E. et al. Linking surface phytoplankton dynamics to small-particle fluxes in the mesopelagic zone: insights from high latitude bioregions using BGC-Argo floats. *Glob. Biogeochem. Cycles* **39**, e2024GB008447 (2025).
11. Giering, S. L. C. et al. High export via small particles before the onset of the North Atlantic spring bloom. *J. Geophys. Res. Oceans* **121**, 6929–6945 (2016).
12. Dall'Olmo, G. & Mork, K. A. Carbon export by small particles in the Norwegian Sea. *Geophys. Res. Lett.* **41**, 2921–2927 (2014).
13. Takeuchi, M. et al. Turbulence mediates marine aggregate formation and destruction in the upper ocean. *Sci. Rep.* **9**, 16280 (2019).
14. Mayor, D. J., Sanders, R., Giering, S. L. C. & Anderson, T. R. Microbial gardening in the ocean's twilight zone: detritivorous metazoans benefit from fragmenting, rather than ingesting, sinking detritus. *BioEssays* **36**, 1132–1137 (2014).
15. Romero-Romero, S. et al. Deep zooplankton rely on small particles when particle fluxes are low. *Limnol. Oceanogr. Lett.* **5**, 410–416 (2020).
16. Shea, C. H. et al. Small particles and heterotrophic protists support the mesopelagic zooplankton food web in the subarctic northeast Pacific Ocean. *Limnol. Oceanogr.* **68**, 1949–1963 (2023).
17. Wojtal, P. K. et al. Deconvolving mechanisms of particle flux attenuation using nitrogen isotope analyses of amino acids. *Limnol. Oceanogr.* **68**, 1965–1981 (2023).
18. Baltar, F. et al. Significance of non-sinking particulate organic carbon and dark CO2 fixation to heterotrophic carbon demand in the mesopelagic northeast Atlantic. *Geophys. Res. Lett.* **37**, L09602 (2010).
19. Herndl, G. J. & Reinthaler, T. Microbial control of the dark end of the biological pump. *Nat. Geosci.* **6**, 718–724 (2013).
20. Stephens, B. M. et al. An upper-mesopelagic-zone carbon budget for the subarctic North Pacific. *Biogeosciences* **22**, 3301–3328 (2025).
21. Baker, C. A., Martin, A. P., Yool, A. & Popova, E. Biological carbon pump sequestration efficiency in the North Atlantic: a leaky or a long-term sink? *Glob. Biogeochem. Cycles* **36**, e2021GB007286 (2022).
22. Ricour, F., Guidi, L., Gehlen, M., DeVries, T. & Legendre, L. Century-scale carbon sequestration flux throughout the ocean by the biological pump. *Nat. Geosci.* **16**, 1105–1113 (2023).
23. Siegel, D. A., DeVries, T., Doney, S. C. & Bell, T. Assessing the sequestration time scales of some ocean-based carbon dioxide reduction strategies. *Environ. Res. Lett.* **16**, 104003 (2021).
24. Francois, R., Honjo, S., Krishfield, R. & Manganini, S. Factors controlling the flux of organic carbon to the bathypelagic zone of the ocean. *Glob. Biogeochem. Cycles* **16**, 34−1−34–20 (2002).
25. Wilson, J. D. et al. The biological carbon pump in CMIP6 models: 21st century trends and uncertainties. *Proc. Natl. Acad. Sci. USA*. **119**, e2204369119 (2022).
26. Henson, S. A., Sanders, R. & Madsen, E. Global patterns in efficiency of particulate organic carbon export and transfer to the deep ocean. *Glob. Biogeochem. Cycles* **26**, GB1028 (2012).
27. DeVries, T. & Weber, T. The export and fate of organic matter in the ocean: new constraints from combining satellite and oceanographic tracer observations. *Glob. Biogeochem. Cycles* **31**, 535–555 (2017).

28. Weber, T., Cram, J. A., Leung, S. W., DeVries, T. & Deutsch, C. Deep ocean nutrients imply large latitudinal variation in particle transfer efficiency. *Proc. Natl. Acad. Sci. USA*. **113**, 8606–8611 (2016).
29. Marsay, C. M. et al. Attenuation of sinking particulate organic carbon flux through the mesopelagic ocean. *Proc. Natl. Acad. Sci. USA*. **112**, 1089–1094 (2015).
30. Guidi, L. et al. A new look at ocean carbon remineralization for estimating deepwater sequestration. *Glob. Biogeochem. Cycles* **29**, 1044–1059 (2015).
31. Henson, S. et al. Effect of sampling bias on global estimates of ocean carbon export. *Environ. Res. Lett.* **19**, 024009 (2024).
32. Claustre, H., Johnson, K. S. & Takeshita, Y. Observing the global ocean with Biogeochemical-Argo. *Annu. Rev. Mar. Sci.* **12**, 23–48 (2020).
33. Liniger, G., Sharp, J. D., Takeshita, Y. & Johnson, K. S. Two decades of increase in Southern Ocean net community production revealed by BGC-Argo floats. *Glob. Biogeochem. Cycles* **39**, e2024GB008371 (2025).
34. García-Jiménez, J., Ruescas, A. B., Amorós-López, J. & Sauzède, R. Combining BioGeoChemical-Argo (BGC-Argo) floats and satellite observations for water column estimations of the particulate backscattering coefficient. *Ocean Sci.* **21**, 1677–1694 (2025).
35. Mignot, A. et al. Using machine learning and Biogeochemical-Argo (BGC-Argo) floats to assess biogeochemical models and optimize observing system design. *Biogeosciences* **20**, 1405–1422 (2023).
36. Cetinić, I. et al. Particulate organic carbon and inherent optical properties during 2008 North Atlantic Bloom Experiment. *J. Geophys. Res. Oceans* **117**, (2012).
37. Koestner, D., Stramski, D. & Reynolds, R. A. Improved multivariable algorithms for estimating oceanic particulate organic carbon concentration from optical backscattering and chlorophyll-a measurements. *Front. Mar. Sci.* **10**, 1197953 (2024).
38. Sauzède, R. et al. A neural network-based method for merging ocean color and Argo data to extend surface bio-optical properties to depth: retrieval of the particulate backscattering coefficient. *J. Geophys. Res. Oceans* **121**, 2552–2571 (2016).
39. Sauzède, R., Renosh, P. R., Schmechtig, C., Uitz, J. & Claustre, H. Global Ocean 3D Particulate Organic Carbon and Chlorophyll-a concentration Product. https://doi.org/10.48670/moi-00046 (2024).
40. Cael, B. B. & Bisson, K. Particle flux parameterizations: quantitative and mechanistic similarities and differences. *Front. Mar. Sci.* **5**, 395 (2018).
41. Oetjens, A., Chase, Z., Strutton, P. & Rohr, T. An improved model of particle attenuation reduces estimates of Southern Ocean carbon transfer efficiency. *Commun. Earth Environ.* **6**, 1041 (2025).
42. Williams, J. A., Henson, S. A., Briggs, N. & Hickman, A. Unexpected global prevalence of mesopelagic particle layers detected by BGC-Argo floats. *Geophys. Res. Lett*.
43. Johnson, L. et al. Assessment of oceanographic conditions during the North Atlantic EXport processes in the ocean from RemoTe sensing (EXPORTS) field campaign. *Prog. Oceanogr.* **220**, 103170 (2024).
44. Stramski, D. et al. Relationships between the surface concentration of particulate organic carbon and optical properties in the eastern South Pacific and eastern Atlantic Oceans. *Biogeosciences* **5**, 171–201 (2008).
45. Balch, W. M., Bowler, B. C., Drapeau, D. T., Poulton, A. J. & Holligan, P. M. Biominerals and the vertical flux of particulate organic carbon from the surface ocean. *Geophys. Res. Lett.* **37**, L22605 (2010).
46. Bol, R., Henson, S. A., Rumyantseva, A. & Briggs, N. High-frequency variability of small-particle carbon export flux in the Northeast Atlantic. *Glob. Biogeochem. Cycles* **32**, 1803–1814 (2018).
47. Palevsky, H. I. & Doney, S. C. How choice of depth horizon influences the estimated spatial patterns and global magnitude of ocean carbon export flux. *Geophys. Res. Lett.* **45**, 4171–4179 (2018).
48. Buesseler, K. O., Boyd, P. W., Black, E. E. & Siegel, D. A. Metrics that matter for assessing the ocean biological carbon pump. *Proc. Natl. Acad. Sci.* **117**, 9679–9687 (2020).
49. Leung, S. W., Weber, T., Cram, J. A. & Deutsch, C. Variable particle size distributions reduce the sensitivity of global export flux to climate change. *Biogeosciences* **18**, 229–250 (2021).
50. Omand, M. M., Govindarajan, R., He, J. & Mahadevan, A. Sinking flux of particulate organic matter in the oceans: Sensitivity to particle characteristics. *Sci. Rep.* **10**, 5582 (2020).
51. Siegel, D. A. et al. Global assessment of ocean carbon export by combining satellite observations and food-web models. *Glob. Biogeochem. Cycles* **28**, 181–196 (2014).
52. Briggs, N., Dall'Olmo, G. & Claustre, H. Major role of particle fragmentation in regulating biological sequestration of CO 2 by the oceans. *Science* **367**, 791–793 (2020).
53. Bellacicco, M., Marullo, S., Dall'Olmo, G., Iudicone, D. & Buongiorno Nardelli, B. The oceanic physical injection pump of organic carbon. *Nat. Commun.* **16**, 7100 (2025).
54. Boyd, P. W., Claustre, H., Levy, M., Siegel, D. A. & Weber, T. Multi-faceted particle pumps drive carbon sequestration in the ocean. *Nature* **568**, 327–335 (2019).
55. Dall'Olmo, G., Dingle, J., Polimene, L., Brewin, R. J. W. & Claustre, H. Substantial energy input to the mesopelagic ecosystem from the seasonal mixed-layer pump. *Nat. Geosci.* **9**, 820–823 (2016).
56. Fay, A. R. & McKinley, G. A. Global open-ocean biomes: mean and temporal variability. *Earth Syst. Sci. Data* **6**, 273–284 (2014).
57. Cael, B. B., Cavan, E. L. & Britten, G. L. Reconciling the size-dependence of marine particle sinking speed. *Geophys. Res. Lett.* **48**, e2020GL091771 (2021).
58. Buitenhuis, E. T. et al. MAREDAT: towards a world atlas of MARine Ecosystem DATa. *Earth Syst. Sci. Data* **5**, 227–239 (2013).
59. Wang, W.-L. et al. Biological carbon pump estimate based on multidecadal hydrographic data. *Nature* **624**, 579–585 (2023).
60. Laufkötter, C., John, J. G., Stock, C. A. & Dunne, J. P. Temperature and oxygen dependence of the remineralization of organic matter. *Glob. Biogeochem. Cycles* **31**, 1038–1050 (2017).
61. Garcia, H. E. et al. World Ocean Atlas 2023, Volume 3: Dissolved Oxygen, Apparent Oxygen Utilization, and Oxygen Saturation. Tech. Ed. NOAA Atlas NESDIS 91. https://doi.org/10.25923/rb67-ns53 (2023).
62. Alcolombri, U. et al. Sinking enhances the degradation of organic particles by marine bacteria. *Nat. Geosci.* **14**, 775–780 (2021).
63. Robinson, C. Microbial respiration, the engine of ocean deoxygenation. *Front. Mar. Sci.* **5**, 533 (2019).
64. Lacour, L., Briggs, N., Claustre, H., Ardyna, M. & Dall'Olmo, G. The intraseasonal dynamics of the mixed layer pump in the subpolar North Atlantic Ocean: a Biogeochemical-Argo float approach. *Glob. Biogeochem. Cycles* **33**, 266–281 (2019).
65. Koestner, D., Stramski, D. & Reynolds, R. A. A multivariable empirical algorithm for estimating particulate organic carbon concentration in marine environments from optical backscattering and chlorophyll-a measurements. *Front. Mar. Sci.* **9**, 941950 (2022).
66. Aumont, O. et al. Variable reactivity of particulate organic matter in a global ocean biogeochemical model. *Biogeosciences* **14**, 2321–2341 (2017).
67. Orihuela-García, M. A. et al. Dissecting mesopelagic particulate organic carbon budgets in the North Atlantic: a mechanistic diagnosis and evaluation of PISCESv2_RC. *Biogeosciences* **23**, 4083–4112 (2026).
68. Steinberg, D. K. et al. Bacterial vs. zooplankton control of sinking particle flux in the ocean's twilight zone. *Limnol. Oceanogr.* **53**, 1327–1338 (2008).
69. Giering, S. L. C. et al. Reconciliation of the carbon budget in the ocean's twilight zone. *Nature* **507**, 480–483 (2014).

70. Bressac, M. et al. Decoding drivers of carbon flux attenuation in the oceanic biological pump. *Nature* **633**, 587–593 (2024).
71. Stukel, M. R., Ohman, M. D., Kelly, T. B. & Biard, T. The roles of suspension-feeding and flux-feeding zooplankton as gatekeepers of particle flux into the mesopelagic ocean in the Northeast Pacific. *Front. Mar. Sci.* **6**, 397 (2019).
72. Stukel, M. R. et al. Mesoscale ocean fronts enhance carbon export due to gravitational sinking and subduction. *Proc. Natl. Acad. Sci. USA*. **114**, 1252–1257 (2017).
73. Levy, M. et al. Physical pathways for carbon transfers between the surface mixed layer and the ocean interior. *Glob. Biogeochem. Cycles* **27**, 1001–1012 (2013).
74. Stukel, M. R., Song, H., Goericke, R. & Miller, A. J. The role of subduction and gravitational sinking in particle export, carbon sequestration, and the remineralization length scale in the California Current Ecosystem. *Limnol. Oceanogr.* **63**, 363–383 (2018).
75. Briggs, N. et al. High-resolution observations of aggregate flux during a sub-polar North Atlantic spring bloom. *Deep Sea Res. Part Oceanogr. Res. Pap.* **58**, 1031–1039 (2011).
76. Edwards, P. et al. Capturing the global variability of marine particulate organic carbon flux: a hierarchical Bayesian approach. *Geophys. Res. Lett.* **53**, e2026GL123203 (2026).
77. Evers-King, H. et al. Validation and intercomparison of ocean color algorithms for estimating particulate organic carbon in the oceans. *Front. Mar. Sci.* **4**, 251 (2017).
78. de Boyer Montégut, C., Madec, G., Fischer, A. S., Lazar, A. & Iudicone, D. Mixed layer depth over the global ocean: an examination of profile data and a profile-based climatology. *J. Geophys. Res. Oceans* **109**, C12003 (2004).
79. Moriarty, R. & O'Brien, T. D. Distribution of mesozooplankton biomass in the global ocean. *Earth Syst. Sci. Data* **5**, 45–55 (2013).
80. Aumont, O., Ethé, C., Tagliabue, A., Bopp, L. & Gehlen, M. PISCES-v2: an ocean biogeochemical model for carbon and ecosystem studies. *Geosci. Model Dev.* **8**, 2465–2513 (2015).
81. Boudreau, B. & Ruddick, B. On a reactive continuum representation of organic matter diagenesis. *Am. J. Sci.* **291**, 507–538 (1991).
82. Henson, S., Sauzède, R., Aumont, O., Giering, S. L. C. & Briggs, N. Dataset and code associated with 'Global patterns in small organic particle loss in the mesopelagic'. https://doi.org/10.5281/zenodo.18418243 (2026).

Acknowledgements

We are grateful to the OneArgo programme whose data form the basis of the BGC-Argo data product used in this study. The data were collected and made freely available by the International Argo Program and the national programs that contribute to it (https://argo.ucsd.edu, https://www.ocean-ops.org). The OneArgo Program is part of the Global Ocean Observing System.

Author contributions

Stephanie Henson conceived the study, undertook the analysis and led writing the manuscript. Raphaëlle Sauzède created the dataset this work is based on, and contributed to writing and editing the manuscript. Olivier Aumont created the versions of the model used here, and contributed to writing and editing the manuscript. Sari Giering contributed to the conceptualisation of the work, and writing and editing the manuscript. Nathan Briggs contributed to the conceptualisation of the work, the methodology, and writing and editing the manuscript.

Funding

S.H. was supported by the CALIPSO (Carbon Loss In Plants, Soils and Oceans) project, funded through the generosity of Eric and Wendy Schmidt by recommendation of the Schmidt Science program. S.H. and N.B. received funding from the Natural Environment Research Council (PARTITRICS, NE/Y004329/1; GLOBESINK, NE/X008657/1) and from the European Union under grant agreement no. 101083922 (OceanICU) and UK Research and Innovation (UKRI) under the UK government's Horizon Europe funding guarantee [grant number 10054454, 10063673, 10064020, 10059241, 10079684, 10059012, 10048179]. S.L.C.G. was supported through the ANTICS project, receiving funding from the European Research Council (ERC) under the European Union's Horizon 2020 research and innovation program (Grant Agreement 950212). Views and opinions expressed are however those of the author(s) only and do not necessarily reflect those of the European Union or European Research Executive Agency. Neither the European Union nor the granting authority can be held responsible for them.

Competing interests

The authors declare no competing interests.

Additional information

Supplementary information The online version contains supplementary material available at https://doi.org/10.1038/s43247-026-03939-5.

Correspondence and requests for materials should be addressed to Stephanie Henson.

Peer review information *Communications Earth & Environment* thanks Guillaume Liniger and the other, anonymous, reviewer(s) for their contribution to the peer review of this work. Primary Handling Editors: Heike Langenberg and Marisa McDonald. A peer review file is available.

Reprints and permissions information is available at http://www.nature.com/reprints

Publisher's note Springer Nature remains neutral with regard to jurisdictional claims in published maps and institutional affiliations.

Open Access This article is licensed under a Creative Commons Attribution 4.0 International License, which permits use, sharing, adaptation, distribution and reproduction in any medium or format, as long as you give appropriate credit to the original author(s) and the source, provide a link to the Creative Commons licence, and indicate if changes were made. The images or other third party material in this article are included in the article's Creative Commons licence, unless indicated otherwise in a credit line to the material. If material is not included in the article's Creative Commons licence and your intended use is not permitted by statutory regulation or exceeds the permitted use, you will need to obtain permission directly from the copyright holder. To view a copy of this licence, visit http://creativecommons.org/licenses/by/4.0/.

© The Author(s) 2026

This Article in Press is shared early to give you faster access to new research. It is citable and carries a permanent DOI. The final edited version will replace it automatically.